



Published in final edited form as:

*J Nutr Biochem*. 2021 December ; 98: 108815. doi:10.1016/j.jnutbio.2021.108815.

## Pterostilbene leads to DNMT3B-mediated DNA methylation and silencing of OCT1-targeted oncogenes in breast cancer cells

Megan Beetch<sup>1,#</sup>, Cayla Boycott<sup>1,#</sup>, Sadaf Harandi-Zadeh<sup>1</sup>, Tony Yang<sup>1</sup>, Benjamin J. E. Martin<sup>2,3</sup>, Thomas Dixon-McDougall<sup>4</sup>, Kevin Ren<sup>1</sup>, Allison Gacad<sup>1</sup>, John H. Dupuis<sup>1</sup>, Melissa Ullmer<sup>5</sup>, Katarzyna Lubecka<sup>6</sup>, Rickey Y. Yada<sup>1</sup>, Carolyn J. Brown<sup>4</sup>, LeAnn J. Howe<sup>2</sup>, Barbara Stefanska<sup>1,\*</sup>

<sup>1</sup>Food, Nutrition and Health Program, Faculty of Land and Food Systems, University of British Columbia, Vancouver, BC, Canada

<sup>2</sup>Department of Biochemistry and Molecular Biology, University of British Columbia, Vancouver, BC, Canada

<sup>3</sup>Department of Biological Chemistry and Molecular Pharmacology, Harvard Medical School, Boston, MA, USA

<sup>4</sup>Department of Medical Genetics, Molecular Epigenetics Group, Life Sciences Institute, University of British Columbia, Vancouver, BC, Canada

<sup>5</sup>Department of Anatomy, Cell Biology and Physiology, Indiana University School of Medicine, Indianapolis, IN, USA

<sup>6</sup>Department of Biomedical Chemistry, Medical University of Lodz, Lodz, Poland

### Abstract

Transcription factor (TF)-mediated regulation of genes is often disrupted during carcinogenesis. The DNA methylation state of TF-binding sites may dictate transcriptional activity of corresponding genes. Stilbenoid polyphenols, such as pterostilbene (PTS), have been shown to exert anti-cancer action by remodeling DNA methylation and gene expression. However, the mechanisms behind these effects still remain unclear. Here, the dynamics between oncogenic TF OCT1 binding and *de novo* DNA methyltransferase DNMT3B binding in PTS-treated MCF10CA1a invasive breast cancer cells has been explored. Using chromatin immunoprecipitation (ChIP) followed by next generation sequencing, we determined 47 gene regulatory regions with decreased OCT1 binding and enriched DNMT3B binding in response to PTS. Most of those genes were found to have oncogenic functions. We selected three candidates, *PRKCA*, *TNNT2* and *DANT2*, for further mechanistic investigation taking into account *PRKCA*

\* **Corresponding Author:** Dr. Barbara Stefanska, Assistant Professor, Faculty of Land and Food Systems, University of British Columbia, 2205 East Mall, FNH 150, Vancouver, BC V6T 1Z4, Phone: +1 604-822-2524, Fax: +1 604-822-5143, barbara.stefanska@ubc.ca, <http://www.landfood.ubc.ca/barbara-stefanska/>.

#first co-authors who equally contributed to this work

**AUTHOR CONTRIBUTIONS:** M.B., C.B., and B.S. conceptualized and designed the study. M.B., C.B., S.H-Z., T.Y., A.G., K.R., M.U., K.L., and B.S. performed experiments and analyzed the data. T.D-M and C.J.B were collaborators on generation of CRISPR DNMT3B knockout cell line. B.J.E.M., L.J.H., J.H.D., and R.Y. were collaborators on the analysis of raw ChIP sequencing data. M.B., C.B., and B.S. wrote the manuscript and prepared the figures. C.B., T.Y., K.R., M.B., S.H-Z., and B.S. revised the manuscript.

**CONFLICTS OF INTEREST:** The authors declare no conflict of interest.

functional and regulatory connection with numerous cancer-driving processes and pathways, and some of the highest increase in DNMT3B occupancy within *TNNT2* and *DANT2* enhancers. PTS led to DNMT3B recruitment within *PRKCA*, *TNNT2*, and *DANT2* at loci that also displayed reduced OCT1 binding. Substantial decrease in OCT1 with increased DNMT3B binding were accompanied by *PRKCA* promoter and *TNNT2* and *DANT2* enhancer hypermethylation, and gene silencing. Interestingly, DNA hypermethylation of the genes was not detected in response to PTS in DNMT3B-CRISPR knockout MCF10CA1a breast cancer cells. It indicates DNMT3B-dependent methylation of *PRKCA*, *TNNT2*, and *DANT2* upon PTS. Our findings provide a better understanding of mechanistic players and their gene targets that possibly contribute to the anti-cancer action of stilbenoid polyphenols.

## Keywords

pterostilbene; oncogenes; DNA methylation; DNMT3B; chromatin; cancer

## 1. INTRODUCTION

DNA methylation is one of the components of the epigenome which strongly dictates the availability for transcriptional machinery, including transcription factors (TFs), to bind DNA and instigate transcription [1, 2]). Specifically, increased methylation of regulatory regions of tumor suppressor genes (TSGs) or decreased methylation of regulatory regions of oncogenes has been found to result in corresponding changes in gene expression, namely silencing of TSGs or upregulation of oncogenes in many cancer types including breast cancer [3–5]. Several groups have identified TFs that are sensitive to DNA methylation status at the recognized elements or their proximity. For instance, TFs such as NRF1, CTCF, NF- $\kappa$ B, CREB, and OCT1 have impaired binding to DNA when cytosines are methylated around their respective TF binding sites [6–11]. Numerous pieces of evidence show that changes in gene expression during carcinogenesis is often related to genes with differentially methylated regions and those regions are enriched for binding sites of methylation-sensitive TFs. Hence, the interplay between DNA methylation and TF binding within regulatory regions of cancer-related genes is of great interest and may at least partially explain the transcriptional dysregulation occurring during carcinogenesis and potential mechanisms of the action of anti-cancer agents, including dietary bioactive compounds [12].

Bioactive compounds present in our diet have been shown to remodel DNA methylation patterns and impact regulation of DNA methylation machinery in cancer models [3, 4, 13]. Specifically, stilbenoid polyphenols, resveratrol (RSV) and its dimethylated analogue pterostilbene (PTS), that are present abundantly in grapes and blueberries, respectively, have been shown to elicit bidirectional effects on DNA methylation status, change binding of DNA methyltransferases (DNMTs), and alter TF occupancy within differentially methylated regions [3, 4]. A classic example is the capacity of RSV to effectively reverse cancer-specific hypermethylation and silencing of numerous TSGs such as *BRCA1*, *RASSF1A*, and *PTEN* [14–16]. Additionally, PTS led to an increase in DNA methylation of the *Fasn* gene promoter, which averted *Fasn* upregulation upon obesogenic diet in rats [17]. Furthermore, using genome-wide technology, we have previously identified differentially methylated

genes in response to RSV and followed up with mechanistic studies to describe epigenetic and transcriptional regulators associated with remodeling of the DNA methylation patterns in response to stilbenoids, RSV and PTS [3, 4]. We were the first group to show that treatment of breast cancer cells with stilbenoids results in DNA hypermethylation of regulatory regions of numerous genes with oncogenic and pro-metastatic functions and silences them. Interestingly, we specifically showed that 80% of regions hypermethylated in response to stilbenoids encompass a putative binding site for OCT1 [3].

OCT1 is a ubiquitous transcription factor that controls a wide range of target genes including genes involved in immune response, metabolic regulation, and stem cell function [18]. OCT1 expression levels are increased in certain malignancies such as gastric, breast, lung, and thyroid cancer and has been suggested to have a role in tumor initiation and progression [19]. Moreover, regions across the genome that are implicated in cancer malignancies have also been shown to be enriched with OCT1 binding sites, and elevated OCT1-mediated transcription is associated with poor prognosis in different cancers [20, 21]. Analysis of the regulatory region in *IL2* gene demonstrated that 90% methylation at a CpG site within OCT1 binding site motif correlates with *IL2* transcriptional inactivity in MCF-7 breast cancer cells [10]. The same CpG site was demethylated in stimulated human T cells that express *IL2* [10]. The sensitivity of OCT1 to DNA methylation within its binding region has also been shown in other genes such as *CDX2*, *DAPK* and *HSPA2* [22–24].

Previously, we have shown that stilbenoid treatment restores DNA methylation at the *MAML2* regulatory enhancer region leading to *MAML2* silencing, which subsequently inhibits tumorigenic properties of breast cancer cells [3]. These changes corresponded with increased binding of DNMT3B, a *de novo* DNMT, and decreased binding of OCT1 within the tested *MAML2* region. Of note, PTS exerted those effects at lower concentrations (7  $\mu$ M) compared with RSV (15  $\mu$ M), which supports the higher bioavailability and metabolic stability of PTS observed by others in *in vivo* studies [25]. These results have given us the basis for focusing on PTS and suggesting that OCT1-targeted oncogenes may be silenced through a mechanism whereby stilbenoid compounds recruit DNMT3B to regulatory regions of oncogenes to increase methylation and consequently reduce transcriptional activity. To further investigate these mechanistic players and their roles in modulating expression of genes with potential oncogenic functions, we have performed chromatin immunoprecipitation (ChIP) followed by next-generation sequencing to analyze binding events of OCT1 and DNMT3B at a genome-wide scale. We then elucidated a DNMT3B-dependent mechanism of hypermethylation and silencing of OCT1-targeted oncogenes which may, at least partially, contribute to the anti-cancer effects of stilbenoid polyphenols.

## 2. MATERIALS AND METHODS

### 2.1. Cell culture and pterostilbene (PTS) treatment

Human breast cancer MCF10CA1a cell lines were cultured in DMEM/F12 (1:1) medium (Gibco) supplemented with 5% horse serum (Gibco), 1U/ml penicillin and 1 $\mu$ g/ml streptomycin (Gibco). MCF10CA1a breast cancer cells were obtained from Dr. Dorothy Teegarden, Purdue University, IN, USA. They were derived from tumor xenografts of

MCF10A cells transformed with constitutively active Harvey-*ras* oncogene, and represent poorly-differentiated malignant tumors. Cell lines were routinely verified by morphology, invasion and growth rates as well as authentication by DNA profiling using the short tandem repeat (ATCC). Cells, grown in a humidified atmosphere of 5% carbon dioxide at 37°C, were treated with pterostilbene (PTS, Cayman Chem., Ann Arbor, MI, USA) freshly resuspended in ethanol. 24 h prior to treatments, cells were plated at a density of  $2-3 \times 10^5$  followed by exposure to PTS at 7µM concentration for 4 days. Cells were then passaged 1:50 and exposed for additional 4 days (9-day exposure). 7µM concentration for a total of 9 days was determined in our previous studies to be the IC50 concentration [3, 4].

## 2.2. Chromatin immunoprecipitation (ChIP) sequencing (ChIP-seq)

Chromatin immunoprecipitation was performed as previously described [3, 26]. Briefly, cells representing three biological replicates were fixed with formaldehyde, incubated with protease inhibitors, lysed and subjected to cycles of sonication. Samples were pre-cleared with protein G agarose followed by centrifugation. Supernatants were divided into three sub-samples. One sub-sample was maintained as input. The second sub-sample served as negative control and was incubated with mouse or rat IgG non-specific antibody (negative control, Santa-Cruz Biotechnology). The third sub-sample was incubated with anti-OCT1 mouse antibody (Millipore, MAB5434) or anti-DNMT3B rat antibody (Millipore, MABE305). The next day, the fraction of DNA bound to antibodies was washed, eluted and used as a template for ChIP-seq and qChIP.

Library preparation was carried out using NEBNext Ultra DNA Library Prep Kit for Illumina reagents according to the manufacturer's protocol. ChIP libraries were sequenced using PE150bp reads in HiSeq2500, as described previously [27, 28]. ChIP-seq data were analyzed using Bioconductor tool in R, as described previously [27, 28]. Adapter sequences were trimmed from sequencing reads using cutadapt [29], and reads were aligned to the GRCh37/hg19 human reference genome using the Burrows-Wheeler Aligner [30]. MACS2 peak calling software was used to identify enrichment patterns in control-treated versus PTS-treated samples [31, 32]. Differential binding was assessed through occupancy analysis and visualized on genome browser. ChIPSeeker Bioconductor package was used to assign peaks to closest gene. The ChIP quality control (CHIPQC) Bioconductor package calculated ChIP-seq specific quality metric for each sample and input in our experiment. CHIPQC further identifies both fragment length peak and a read length peak based on cross-coverage around the centers of binding sites. CHIPQC was used to both measure inequality of coverage across the genome via standardized Standard Deviation (SSD) and assess distribution of ChIP-seq signal over genomic regions.

Broad ChromHMM data from human mammary epithelial cells (HMEC) were used to assign peaks to chromatin states [33]. Peaks could correspond to the following chromatin states: active, weak or poised promoters, strong or weak enhancers, putative insulators, active or weak transcription, Polycomb-repressed regions or heterochromatin. Active promoters, strong enhancers and active transcription regions are linked to high expression levels, with the latter state determined based on the enrichment of histone marks along

transcripts. The ChIP-seq data are available from Gene Expression Omnibus (accession numbers: GSE175639).

ChIP DNA at an amount of 25ng of input, antibody bound and IgG bound DNA was used as starting material in all conditions. Levels of OCT1 and DNMT3B binding were expressed as (Bound-IgG)/Input. Primers used in qChIP are listed in Supplementary Table S1.

### 2.3. DNA isolation and pyrosequencing

DNA, isolated using standard phenol:chloroform extraction protocol, was treated with sodium bisulfite as previously described [3]. HotStar Taq DNA polymerase (Qiagen) and biotinylated primers were used to amplify bisulfite converted promoter region of *PRKCA* and enhancer regions of *TNNT2* and *DANT2* (please see Supplementary Table S1 for primer sequences). Pyrosequencing of the biotinylated DNA strands was performed in the PyroMark Q48 Autoprep instrument (Qiagen). Percentage of methylation at a single CpG site resolution was calculated using PyroMark Q48 software.

### 2.4. RNA isolation and qPCR

TRIzol (Invitrogen) was used to isolate total RNA which served as a template for cDNA synthesis with AMV reverse transcriptase (Roche Diagnostics), according to the manufacturer's protocol. Amplification reaction was performed in CFX96 Touch Real-Time PCR Detection System (Bio-Rad) using 2 µl of cDNA, 400 nM forward and reverse primers (please see Supplementary Table S1 for sequences), and 10 µl of SsoFast EvaGreen Supermix (Bio-Rad) in a final volume of 20 µl. The following cycles were used in the amplification reaction: denaturation at 95 °C for 10 min, amplification for 60 cycles at 95 °C for 10s, annealing temperature for 10s, 72 °C for 10s, and final extension at 72 °C for 10 min. The CFX Maestro Software (Bio-Rad) was used to quantify gene expression with a standard curve-based analysis. qPCR data is presented as gene of interest/GAPDH (reference gene).

### 2.5. CRISPR-Cas9 knockout of DNMT3B in MCF10CA1a cells

Online tool E-Crisp was used to design gRNAs targeting the first or second exon of the DNMT3B gene. The gRNA was cloned into pSPgRNA (Plasmid #47108, Addgene, a gift from Charles Gersbach [34]), and transformed into Subcloning Efficiency™ DH5α™ Competent Cells (Life Technologies). The transfection protocol was performed with Lipofectamine 3000 according to the instructions using pCAS9-mCherry-Frame+0 (Plasmid #66939, Addgene, a gift from Veit Hornung [35]) and a CRISPaint plasmid pCRISPaint-TagGFP2-PuroR from the CRISPaint Gene Tagging Kit (Plasmid #80970, Addgene, a gift from Veit Hornung [35]). MCF10CA1a cells were transfected with a 1:1:2 mass ratio of gRNA, Cas9 and donor into 24 well plates. Selection in puromycin for 5 days was initiated 48 hours after transfection at a concentration of 1.5µg/ml. Cells were then picked and grown before being tested by PCR and subjected to further experiments.

### 2.6. Western blot

Total protein extract was obtained using RIPA buffer. Samples were subjected to electrophoresis in fast cast SDS-PAGE gels according to the manufacturer's protocol (Bio-

Rad). Next, the separated proteins were transferred onto a TransBlot Turbo Polyvinylidene Fluoride (PVDF) membrane using a Trans-Blot Turbo Transfer System (Bio-Rad). PVDF membranes were imaged on the Bio-Rad ChemiDoc imaging system to verify transfer. Membranes were blocked in EveryBlot Blocking Buffer for 5 min at room temperature and then incubated overnight at 4 °C with the primary monoclonal antibody, anti-DNMT3B (1:2000; MABE305, Millipore). The membranes were then incubated for 1 h at room temperature with secondary antibody horseradish peroxidase-conjugated anti-rat IgG (1:5000; AP136P, Millipore). After incubation, the blots were imaged on a Bio-Rad ChemiDoc imaging system in order to measure total protein content as a loading control for protein normalization, as previously described [36]. Membranes were developed with the Clarity Western ECL Substrate (Bio-Rad), chemiluminescent signals were acquired on ChemiDoc MP (Bio-Rad) and band intensities were analyzed using Image Lab software (Bio-Rad).

## 2.7. Statistical analysis

Unpaired *t*-test with two-tailed distribution was used for statistical analysis of pyrosequencing, qPCR, and qChIP quantitative data. Each value represents the mean  $\pm$  S.D. of three independent experiments. The results were considered statistically significant when  $P < 0.05$ .

## 3. RESULTS

### 3.1. Overview of genome-wide changes in OCT1 binding in response to pterostilbene (PTS)

To understand how stilbenoid polyphenols impact genes recognized and bound by OCT1, we performed ChIP with OCT1-specific antibody followed by next-generation sequencing in MCF10CA1a breast cancer cells upon treatment with 7  $\mu$ M PTS for 9 days. This specific PTS concentration was determined as the IC50 concentration for MCF10CA1a cells in our previous work [3]. IC50 refers to a non-toxic dose (less than 10% of dead cells) that causes 50% inhibition in cell growth compared with control (cells treated with ethanol as vehicle) [3, 4]. OCT1 binding significantly changes in 7,087 regions (peaks) throughout the genome in response to PTS (Figure 1A). Almost 65% of those changes (4,587 peaks) represent OCT1-reduced peaks where OCT1 binding decreases upon PTS as compared with control cells (Figure 1A). Since our previous work on *MAML2* enhancer suggested the role of OCT1 in stilbenoid-mediated epigenetic silencing of potential oncogenes [3], we focused on peaks with lower OCT1 occupancy in the present investigation.

Chromosomal view of peaks with reduced OCT1 binding in response to PTS was plotted using Integrative Genome Viewer (IGV) visualization tool in Figure 1B. Each bar represents a single peak that was called using MACS2 peak calling method. Peaks were aligned to the closest gene using the hg19 human genome and assigned to chromatin states based on Broad ChromHMM tracks from human mammary epithelial cells (HMEC) (Figure 1C). A total of 3,994 OCT1-reduced peaks were assigned to different chromatin states with the rest falling into a category of unassigned. A majority of the peaks were situated within gene regulatory regions, with 17% of them in promoters and enhancers (Figure 1C). Those 763 peaks in

promoters and enhancers corresponded to 326 unique genes. As promoters and enhancers are directly associated with transcriptional regulation and OCT1, as a transcription factor, binds to the octamer motif (ATGCAAAT) or closely related sequences in promoters and enhancers of a variety of genes, we further explored these regions and corresponding genes.

Functional and signaling pathway analyses revealed that the 326 genes, that we refer to as “OCT1-bound PTS target genes” in the following sections, are associated with cell growth and cell cycle regulation, cell adhesion, apoptosis, and positive regulation of cell motility (Figure 1D). Many genes are implicated in signaling pathways that are commonly activated during cancer development and progression, e.g., *MAP2K3*, *GAPVD1* and *RASD1* (MAP-kinase mediated signaling cascade), *RACK1* (ERK and TNF signaling), *LAMTOR2* and *RRAGA* (MAPK and mTOR signaling), and *PRKCA* (NFκB, MAPK and PI3K-AKT signaling) (Figure 1D). Indeed, a thorough analysis demonstrated many candidates with oncogenic functions. Several genes were found to be involved in DNA damage and immune response (*FCGR2A*, *NOS1AP*, *PRDX6*, *ASCC1*, *G3BP1*, and *HAUS6*), others with protein folding/trafficking (*DNAJB12*, *FBXW11*, *ANKHDI1*, and *SH3RF2*) and mitochondrial functions and metabolism regulation (*MCU*, *SIGMAR1*, *SHMT1*, and *MICU1*). There were also genes associated with transcriptional activity such as *MYC*, *MLLT3*, *DDX46*, *GLIS3*, *JADE2*, *ANP32E*, *UBE2B*, *CXXC5*, *NR3C1*, *CHD1L*, *ZBTB20*, *PVT1*, and *TLE1*. These findings support our hypothesis that target genes at which OCT1 binding is reduced in response to PTS are mostly associated with cancer-driving functions. The reduction in OCT1 binding within regulatory regions of these oncogenes could contribute to the anti-cancer effects of PTS via decreased transcriptional activity of these cancer-promoting genes.

In line with our findings regarding OCT1 targeting of oncogenes, OCT1 overexpression has been observed in several cancer types such as breast (1.4-fold), esophageal (4.1-fold), cervical (2-fold), gastric (2-fold), and liver (1.6-fold), according to OncoPrint data depicting OCT1 expression levels in human tissues (Figure 1E). Several other pieces of evidence have confirmed OCT1 as an oncogenic transcription factor [19]. Additionally, our past studies show that siRNA depletion of OCT1 in MCF10CA1a invasive breast cancer cells leads to significant reduction in cancer cell growth [3]. Taking into account the oncogenic role of OCT1 and its gene targets, understanding the ways to reduce OCT1-mediated regulation of transcription may contribute to effective anti-cancer strategies.

### 3.2. PTS-induced changes in DNMT3B binding within OCT1-reduced peaks located at promoters and enhancers

As mentioned previously, binding of TFs to regulatory regions of genes can be altered by the DNA methylation status at the TF binding site or at a surrounding region. We previously found that DNMT3B binding in an OCT1 binding site upon PTS treatment was associated with reduced OCT1 occupancy, DNA hypermethylation and silencing of the *MAML2* oncogene [3]. Therefore, we performed ChIP with DNMT3B-specific antibody followed by high throughput sequencing to delineate PTS-induced changes in DNMT3B binding, especially at OCT1-reduced peaks within “OCT1-bound PTS target genes”. Out of 3,314 changes detected, DNMT3B binding was enriched at 1,939 peaks with 201 peaks located in promoters and enhancers (Figure 1F). Fifty-six of those DNMT3B-enriched peaks

in promoter/enhancer lost OCT1 binding in response to PTS and corresponded to 39 genes. There were another 8 genes that overlapped between genes with DNMT3B-enriched and OCT1-reduced peaks within promoter/enhancer (total 47 genes) (Figure 1F). However, the distance between the OCT1-reduced peak and the DNMT3B-enriched peak in those 8 genes was larger than 500 base pairs.

Among the total 47 overlap genes, 36 genes contained OCT1-reduced and DNMT3B-enriched peaks within their enhancers, while 9 genes had the peaks in their promoters (Figure 1G). Another 2 genes, *PRKCA* and *NBPF1*, had overlapping peaks in both enhancer and promoter regions (Figure 1G). Interestingly, the highest 13-fold increase in DNMT3B and the highest 19-fold decrease in OCT1 binding was detected within an enhancer region of *DANT2* in response to PTS treatment (Figure 2A). *DANT2* is identified to be one of the macrosatellite repeat, *DXZ4* associated non-coding transcripts [37, 38]. Although *DANT2* function is not well-defined, it is believed to regulate constitutive heterochromatin formation at *DXZ4* [38]. Thus, aberrant expression of *DANT2* may be responsible for alternate chromatin configurations of *DXZ4* in response to cancer [37, 38]. The second highest 12.5-fold increase in DNMT3B binding in response to PTS was located within an enhancer of *TNNT2* (Figure 2A). *TNNT2* was also among top 10 genes with the highest magnitude of OCT1 reduced occupancy (7.6-fold decrease, Figure 2A). Of note, overexpression of *TNNT2* has been shown to be aberrantly amplified in breast cancer and neuroendocrine prostate cancer, suggesting a potential oncogenic role of *TNNT2* [39].

Thorough analysis of other overlap genes revealed many associated with oncogenic and pro-metastatic functions. Indeed, 35 of the 47 genes were associated with established or potential cancer-driving properties, including *NOTCH2NL* that activates Notch signaling by direct interaction with *NOTCH2*, thereby promoting proliferation and self-renewal [40], *PVT1* that is a long non-coding RNA commonly overexpressed in breast cancer and implicated in regulation of *MYC* [41], *CCAT1* that is a long non-coding RNA upregulated in breast cancer and associated with activation of WNT signaling [42], and *ASCC1* that is involved in DNA damage repair [43]. There were also two very strong cancer-related genes, namely *MYC* and *PRKCA*. *MYC* is a pervasive proto-oncogene and transcription factor commonly dysregulated in many cancer types [44], whereas *PRKCA* encodes for protein kinase C alpha (PKC-alpha) responsible for phosphorylation of many protein targets and activation of various cancer-promoting pathways such as the MAPK cascade and the PI3K-AKT pathway [45]. Other interesting oncogenes were *CPLX2* that is upregulated and used as a prognostic marker in various cancer types [46], and *SREPF1*, a gene involved in lipid metabolism [47]. Of note, a link between lipid homeostasis and tumor growth has been identified in several cancer types [48, 49] and downregulation of *SREBF1* was shown to suppress liver tumor growth [47].

We selected three of these oncogenes, namely *PRKCA*, *DANT2* and *TNNT2*, for further investigation to better understand whether the proposed mechanistic players, OCT1 and DNMT3B, are affecting DNA methylation patterns and transcriptional activity in response to PTS. These three candidates are of particular interest. Firstly, *PRKCA* contains overlapping peaks in both promoter and enhancer (Figure 1G), and regulates a network of cancer-driving genes and pathways [45, 50, 51]. Secondly, *DANT2* and *TNNT2* contain DNMT3B-

enriched and OCT1-reduced peaks with the highest or one of the highest magnitude of change upon treatment with PTS (Figure 2A).

### 3.3. DNMT3B occupancy at an OCT1-reduced binding site is accompanied by *PRKCA*, *DANT2* and *TNNT2* hypermethylation and transcriptional silencing

*PRKCA* contains two overlapping peaks with increased DNMT3B and reduced OCT1 occupancy. Since the region within *PRKCA* promoter is CpG rich, it was selected for further mechanistic investigation (Figure 2), along with enhancer regions of *DANT2* and *TNNT2* (Figure 3).

Enrichment with OCT1 and DNMT3B within the tested regions of *PRKCA*, *DANT2*, and *TNNT2* in control MCF10CA1a breast cancer cells (vehicle-treated, blue peaks) and MCF10CA1a cells treated with PTS (red peaks), as determined by ChIP-seq, is visualized in Figure 2B for *PRKCA* and Figure 3A–B for *DANT2* and *TNNT2* (sequencing tracks). As mentioned in the previous paragraph and depicted in Figure 2A, *DANT2* and *TNNT2* were the top genes with the greatest reductions in OCT1 binding along with the highest increases in DNMT3B binding upon PTS. Changes in *PRKCA* promoter region were modest with 4.5-fold decrease in OCT1 occupancy and 4.4-fold DNMT3B enrichment. Hence, we performed quantitative ChIP to confirm the ChIP-seq readings for *PRKCA*. In line with ChIP-seq, quantitative ChIP demonstrated a robust 95% reduction of OCT1 binding and 48% increased in DNMT3B occupancy within *PRKCA* promoter in response to PTS (Figure 2C).

The detected changes in the interaction of OCT1 and DNMT3B with DNA at the regulatory regions of the selected genes could suggest DNA hypermethylation and transcriptional silencing of the genes. Using pyrosequencing, we measured DNA methylation within regions corresponding to differential peaks identified in ChIP-seq (please refer to the gene maps in Figure 2 and Figure 3 for the exact location of analysed CpG sites). Significant hypermethylation of 7 out of 9 CpGs sites within *PRKCA* promoter was detected, with DNA methylation increasing approximately by 10% across all CpGs (Figure 2D). DNA hypermethylation in this region corresponded to 25% decrease in expression of *PRKCA* upon PTS treatment (Figure 2E). We next surveyed for known downstream targets of *PRKCA*-encoded PKC- $\alpha$  kinase, and focused on those targets that are upregulated at mRNA level together with *PRKCA* increased expression (e.g., in breast cancer cells transitioning from epithelial to mesenchymal phenotype) [52]. Interestingly, the decrease in *PRKCA* expression in response to PTS was linked to downregulation of several PKC- $\alpha$ -targets, such as vinculin (*VCL*), FOS Like 1 AP-1 transcription factor subunit (*FOSL1*), and annexin A2 (*ANXA2*), indicating functional relevance of PTS-mediated epigenetic silencing of *PRKCA* (Figure 2F).

*DANT2* enhancer region was hypermethylated across 7 CpG sites with the highest 42% increase in DNA methylation at CpG5 (Figure 3C). These changes corresponded to 43% decrease in *DANT2* expression levels upon PTS treatment (Figure 3D). We also observed that PTS led to the strongest 88% downregulation of *TNNT2* (Figure 3F) which was accompanied by 10% increase in DNA methylation across two CpG site at *TNNT2* enhancer region (Figure 3E).

### 3.4. PTS-mediated hypermethylation of *PRKCA*, *DANT2* and *TNNT2* is dependent on DNMT3B

To determine whether the effect of PTS on DNA methylation within *PRKCA* promoter and *DANT2* and *TNNT2* enhancer regions was specifically through changes in DNMT3B-DNA interactions, we generated a CRISPR-Cas9 knockout MCF10CA1a cell line for *DNMT3B* (DNMT3B KO). Knockout of *DNMT3B* was confirmed at both mRNA and protein levels (Figure 4A and 4B). We treated DNMT3B KO cells for 9 days with PTS at doses ranging from 5  $\mu$ M to 10  $\mu$ M. We found that the IC50 dose of 7  $\mu$ M for MCF10CA1a cells was maintained in DNMT3B KO cells (Figure 4C). Importantly, in response to PTS treatment, none of the CpG sites in the tested *PRKCA*, *DANT2* and *TNNT2* regions showed hypermethylation in DNMT3B KO cells (Figure 4D–F), supporting our hypothesis that PTS-mediated hypermethylation of regulatory regions of oncogenes occurs through a DNMT3B-controlled mechanism. The lack of DNMT3B and hence no DNA hypermethylation at the regulatory regions led to abolishing the suppressive effect of PTS on expression of *DANT2* and *TNNT2* (Figure 4E and 4F, right panels). However, as shown in Figure 4D (right panel), despite the lack of increased DNA methylation, a significant decrease in *PRKCA* expression is observed in DNMT3B KO cells treated with PTS. This finding suggests that PTS is likely also working through other, presumably DNA methylation-independent, mechanisms to regulate *PRKCA* expression, potentially through histone modifications or indirectly through inhibition of oncogenic pathways, especially in the background of effects caused by *DNMT3B* knockout.

Interestingly, *DNMT3B* knockout itself led to downregulation of all three oncogenes leading to 40% decrease in *PRKCA*, 96% reduction of *DANT2*, and 88% decrease in *TNNT2* expression (Supplementary Figure S1A), which is reflected in apparent anti-cancer effects of *DNMT3B* knockout. DNMT3B KO cells grew at a rate of about 30% of original wild-type MCF10CA1a cells and had characteristics that resemble normal breast cells (i.e., growing in multi-layers and stronger anchorage-dependent growth).

Downregulation of the three oncogenes could not be fully explained by hypermethylation of the regulatory regions of those genes (Supplementary Figure S1B). Only 2–4% increases in DNA methylation at several CpGs within *PRKCA*, *DANT2*, and *TNNT2* were detected in DNMT3B KO cells as compared with MCF10CA1a wild-type cells (Supplementary Figure S1B). There may be a mechanism involved that is activated by *DNMT3B* knockout to signal silencing of the oncogenes and the slight hypermethylation at the regulatory regions may be a consequence of such a signaling mechanism. The slight increase in DNA methylation observed within *PRKCA* promoter, and *DANT2* and *TNNT2* enhancers may presumably be catalyzed by another member of DNMT family, although no increase in expression of *DNMT1* or *DNMT3A* was detected. Both *DNMT1* and *DNMT3A* were actually found to be 50% less expressed in DNMT3B KO cells than in wild-type MCF10CA1a cells (Supplementary Figure S1C), despite the targeting specificity of CRISPR-Cas9 technology as determined by guide RNA sequence. Previous studies showed a similar effect of *DNMT3B* knockdown on other DNMTs [53], which could be linked to a strong interaction and cooperation of the members of the DNMT family [54].

### 3.5. OCT1 depletion reduces expression of *PRKCA*, *DANT2*, and *TNNT2* with no changes in DNA methylation

To determine the role of OCT1 in regulation of *PRKCA*, *DANT2*, and *TNNT2* transcription, we tested expression of the genes in MCF10CA1a cells with siRNA-mediated OCT1 depletion which were generated in our previous study [3]. OCT1 depletion resulted in downregulation of all three tested genes (Supplementary Figure S2A). Of note, the changes in expression were not linked to hypermethylation within regulatory regions of those genes (Supplementary Figure S2B). This would suggest that DNA hypermethylation observed upon PTS treatment is not signalled by OCT1-reduced binding. Instead, PTS affects DNMT3B recruitment which results in DNA hypermethylation and OCT1 reduced occupancy, leading to gene silencing.

## 4. DISCUSSION

It has been shown that transcription factor binding activity can be associated with the dynamic changes in local DNA methylation state within and in proximity of binding motifs which is critical in gene regulation in both normal and cancer cells [11]. The mechanisms by which dietary compounds induce modifications in DNA methylation patterns and subsequently change the expression of genes involved in carcinogenesis are an area of great interest. A previous study from our group suggests that hypermethylation of OCT1 binding motifs could play a mechanistic role in stilbenoid-mediated epigenetic inactivation of genes with oncogenic functions [3]. This is in line with the oncogenic role of OCT1 transcription factor that has been shown to be overexpressed in human cancers (Figure 1E) and be involved in upregulation of numerous oncogenic targets and in driving the malignancy of a number of different cancers [19]. Further elaboration on *MAML2*, one of the oncogenes downregulated by stilbenoids, demonstrated that hypermethylation of OCT1 binding site is accompanied by increased DNMT3B presence [3]. In the current study, our goal was to understand the epigenetic regulation of oncogenes exerted by stilbenoids and the mechanistic role of DNMT3B in this regulation. We therefore established OCT1 and DNMT3B occupancy in highly invasive MCF10CA1a breast cancer cells upon 9-day treatment with PTS, using ChIP-seq technology.

In the present study, we show that PTS leads to reduced OCT1 binding in thousands of DNA loci and 17% of the reduced peaks are located in promoters and enhancers assigned to 326 genes (Figure 1C and 1F). The functional analysis of the genes clearly demonstrates functions linked to positive regulation of cell growth, cell cycle progression, cell motility, transcription and oncogenic signaling (e.g., MAPK, mTOR, PI3K-AKT) (Figure 1D).

Forty-seven genes with OCT1-reduced peaks in promoter/enhancer also contained DNMT3B-increased peaks and thus they constitute “OCT1-bound PTS target genes” that are potentially regulated by DNA methylation and DNMT3B specifically (Figure 1F). Three of those candidate genes were selected for further mechanistic investigations, including *DANT2* and *TNNT2*, with the highest or one of the highest magnitudes of change in overlapping DNMT3B enrichment and OCT1 reduction in response to PTS, and *PRKCA*, characterized by strong oncogenic functions [45, 50, 51] and overlapping DNMT3B and OCT1 peaks in its promoter and enhancer (Figure 1G). In response to PTS treatment, we

observed DNA hypermethylation of the *PRKCA* promoter (Figure 2D), and the *DANT2* and *TNNT2* enhancer regions (Figure 3C and 3E) at loci where a decrease in OCT1 binding and an enrichment in DNMT3B occupancy were detected (Figure 2B and 2C, Figure 3A and 3B). This increase in DNA methylation was accompanied by downregulation of gene transcriptional activity (Figure 2E and Figure 3D and 3F). As PKC- $\alpha$ , encoded by *PRKCA*, is implicated in regulation of many processes and signaling pathways, we tested the effects of PTS on several targets. As indicated in Figure 2F, PTS treatment led to a decrease in expression of genes activated by PKC- $\alpha$ , demonstrating that PTS-mediated epigenetic silencing of *PRKCA* is biologically relevant.

Detected hypermethylation and simultaneous DNMT3B enrichment suggest the role for DNMT3B in catalyzing DNA methylation of *PRKCA*, *DANT2*, and *TNNT2*. Indeed, knockout of *DNMT3B* resulted in abolishing hypermethylation of the tested regions upon treatment with PTS (Figure 4D, 4E, and 4F, left panels). This finding mechanistically demonstrates DNMT3B-mediated deposition of methyl marks at the tested OCT1-binding sites upon PTS treatment. Importantly, there are pieces of evidence indicating that DNMT3B targets genes with oncogenic functions for methylation and silencing. For instance, gradual promoter demethylation and re-expression of proto-oncogene *Ment* was observed upon ablation of Dnmt3b function in a mouse model of T-cell lymphomagenesis [55]. Zheng and colleagues similarly reported that *Dnmt3b* deletion results in upregulation of genes with oncogenic functions in a cancer mouse model [56]. Interestingly, in human normal cells, namely primary epidermal keratinocytes, overexpression of *DNMT3B* was shown to lead to methylation and downregulation of *VAV3*, an oncogene involved in the regulation of actin cytoskeletal and gene transcription [57].

Since there was no DNA hypermethylation at *DANT2* and *TNNT2* enhancers in DNMT3B KO cells in response to PTS, no significant downregulation of *DANT2* and *TNNT2* was detected (Figure 4E and 4F, right panels). This result confirms that DNMT3B action is relevant in association with DNA methylation for the regulation of the *DANT2* and *TNNT2* expression after PTS treatment. However, *PRKCA* was suppressed by PTS in DNMT3B KO cells despite the lack of promoter hypermethylation (Figure 4D). We suggest that PTS works through an additional mechanism to turn off *PRKCA*; a mechanism that may be activated by anti-cancer effects caused by *DNMT3B* knockout in MCF10CA1a breast cancer cells. Such a mechanism could involve regulation of other epigenetic components such as histone modifications to change the chromatin state at the *PRKCA* promoter region. Indeed, a recent report demonstrates that *PRKCA* transcription is upregulated by histone demethylase PHF8 that acts to demethylate lysine 27 and lysine 9 of histone H3 [58]. Interestingly, methylation of histone H3 has been shown to be associated with Polycomb complex for repression as well for recruitment of *de novo* DNA methyltransferases [59]. Hence, PTS could possibly repress *PRKCA* by increasing histone H3 methylation and therefore recruiting *DNMT3B*. Another possibility could be linked to indirect effects on *PRKCA* expression through PTS-mediated inhibition of oncogenic signaling pathways in the background of *DNMT3B* knockout. Of note, *DNMT3B* knockout leads to reduced expression of all tested oncogenes (Supplementary Figure S1A). This effect is accompanied by a slight increase in DNA methylation of the regulatory regions of those genes (Supplementary Figure S1B), implying the involvement of other anti-oncogenic effects regulating gene expression. Interestingly,

other research groups previously reported DNA methylation-independent anti-oncogenic effects of *DNMT3B* knockdown and *DNMT3B* knockout [54, 60, 61]. Based on the robust growth suppression, change in morphology of DNMT3B KO cells, and downregulation of the tested oncogenes, as compared to parent MCF10CA1a breast cancer cells, we speculate that overall DNMT3B plays an oncogenic role in these cells and DNMT3B knockout has a broad range of anti-cancer effects with multiple mechanisms involved. Indeed, most studies reported upregulation of *DNMT3B* in breast cancer and *DNMT3B* overexpression was considered as an independent and unfavorable prognostic factor [62–64]. Additionally, reduced cell proliferation was also reported in breast cancer [53, 65], melanoma [61], and colon cancer cells [54, 60] upon *DNMT3B* depletion. However, in several other cancer types, DNMT3B has been shown to silence target oncogenes, thus acting as a tumor suppressor [56, 57, 64]. This contradictory evidence indicates that DNMT3B plays different roles in transcriptional regulation that are context-dependent and determine its oncogenic or tumor suppressor properties [64], which will be explored in our future studies.

Since *DNMT3B* knockout produces anti-cancer effects in breast cancer cells in our current study and other published reports [53, 65], PTS-mediated recruitment of DNMT3B to methylate and silence oncogenes seems to be contradictory to the oncogenic function of DNMT3B. It could potentially suggest that oncogenic or tumor suppressor action of DNMT3B is gene- and loci-specific. Importantly, we want to emphasize that PTS acts as an anti-oxidant [66] and oxidative stress was shown to cause loci-specific aberrations in DNA methylation through activation of DNA repair mechanisms and re-location of DNMTs, including DNMT3B [67, 68]. Thus, PTS, by decreasing oxidative stress, may change DNMT3B occupancy and restore original interactions with DNA [69]. This novel and interesting concept remains to be elucidated.

Changes in DNA methylation at OCT1-binding sites and decrease in OCT1 occupancy upon PTS could suggest a pivotal role of OCT1 in PTS-mediated recruitment of DNMT3B and epigenetic silencing of the tested oncogenes. Interestingly, it was reported that OCT1 associates with histone 3 lysine 9 (H3K9) demethylase Jmjd1a to remove repressive H3K9 dimethylation mark (H3K9me2) [70, 71]. Low levels of H3K9me2, in turn, reduce the affinity of DNMTs to bind and methylate DNA near the OCT1 binding site, particularly in malignant cells [24]. However, it is unclear whether OCT1 governs DNMT3B-DNA interaction and DNA methylation in response to PTS in our study. To address the timeline of events involving binding of OCT1 and DNMT3B, we performed studies in MCF10CA1a cells with depleted OCT1. We showed that the lack of OCT1 does not lead to changes in DNA methylation at regulatory regions of *PRKCA*, *DANT2*, and *TNNT2* (Supplementary Figure S2B). Hence, our findings indicate that the loss of OCT1 binding is rather not a prerequisite for DNMT3B action. Nevertheless, depletion of OCT1 led to downregulated expression of the genes, thus confirming the role of OCT1 in the transcriptional activity (Supplementary Figure S2A). Another interesting observation was that OCT1 depletion decreased gene expression to a lesser extent than PTS treatment (Figure 2E, 3D and 3F for PTS vs. Supplementary Figure S2A for siOCT1). It may indicate that DNA hypermethylation in response to PTS is relevant and contributes to a stronger suppressive signal than just OCT1 depletion.

Based on our findings, we hypothesize that upon PTS exposure DNMT3B binds to the regulatory regions of oncogenes, catalyzes methylation of OCT1 binding sites, and as a result OCT1 cannot recognize its binding site and cannot participate in activation of transcription. As a consequence, a given gene is silenced. Indeed, other studies have demonstrated that cells with loss of *de novo* DNMTs contain hypomethylated regulatory regions that are enriched with OCT1 binding motifs [12]. It has also been shown that the use of DNMT inhibitors such as 5-aza-2'-deoxycytidine decreases the methylation status of OCT1-targeted gene regulatory regions, such as the *STAT4* promoter region containing OCT1 binding motifs, which directly upregulates gene expression [72].

In summary, our results demonstrate a potential mechanistic link between OCT1 and DNMT3B in hypermethylation of regulatory regions of genes with potential cancer-promoting functions in response to PTS treatment. Such epigenetic silencing of oncogenes may be an important contributor to the anti-cancer action of stilbenoid polyphenols. Insights into the mechanistic underpinnings of bioactive compounds eliciting anti-cancer effects are crucial in the development of effective cancer prevention strategies and novel approaches in support of existing therapies.

## Supplementary Material

Refer to Web version on PubMed Central for supplementary material.

## Funding sources:

This research was supported by the University of British Columbia VP Academic (#10R76632) Award, Canadian Foundation for Innovation John R. Evans Leadership Fund and BC Knowledge Development Fund (#37105), and Natural Sciences and Engineering Research Council Discovery Grant (RGPIN-2021-02969) and Discovery Launch Supplement (DGEGR-2021-00286), granted to B.S.; by grants to L.J.H. from the Canadian Institutes of Health Research (PJT-162253) and Natural Sciences and Engineering Research Council (RGPIN-2018-04907); by a grant to R.Y.Y. from the Natural Sciences and Engineering Research Council (RGPIN-2018-04598); and by a grant to C.J.B. from the Canadian Institutes of Health Research (PJT-156048). B.J.E.M. and J.H.D. were supported by fellowships from the Natural Sciences and Engineering Research Council. Kevin Ren was supported by the Undergraduate Student Research Award from the Natural Sciences and Engineering Research Council.

## REFERENCES:

- [1]. Tsai HC, Baylin SB. Cancer epigenetics: linking basic biology to clinical medicine. *Cell research*. 2011;21:502–17. [PubMed: 21321605]
- [2]. Martin EM, Fry RC. Environmental Influences on the Epigenome: Exposure- Associated DNA Methylation in Human Populations. *Annual review of public health*. 2018;39:309–33.
- [3]. Lubecka K, Kurzava L, Flower K, Buvala H, Zhang H, Teegarden D, et al. Stilbenoids remodel the DNA methylation patterns in breast cancer cells and inhibit oncogenic NOTCH signaling through epigenetic regulation of MAML2 transcriptional activity. *Carcinogenesis*. 2016;37:656–68. [PubMed: 27207652]
- [4]. Beetch M, Lubecka K, Shen K, Flower K, Harandi-Zadeh S, Suderman M, et al. Stilbenoid-Mediated Epigenetic Activation of Semaphorin 3A in Breast Cancer Cells Involves Changes in Dynamic Interactions of DNA with DNMT3A and NF1C Transcription Factor. *Molecular nutrition & food research*. 2019;63:e1801386. [PubMed: 31327173]
- [5]. Stefanska B, Huang J, Bhattacharyya B, Suderman M, Hallett M, Han ZG, et al. Definition of the landscape of promoter DNA hypomethylation in liver cancer. *Cancer research*. 2011;71:5891–903. [PubMed: 21747116]

- [6]. Domcke S, Bardet AF, Adrian Ginno P, Hartl D, Burger L, Schubeler D. Competition between DNA methylation and transcription factors determines binding of NRF1. *Nature*. 2015;528:575–9. [PubMed: 26675734]
- [7]. Maurano MT, Wang H, John S, Shafer A, Canfield T, Lee K, et al. Role of DNA Methylation in Modulating Transcription Factor Occupancy. *Cell reports*. 2015;12:1184–95. [PubMed: 26257180]
- [8]. Sunahori K, Juang YT, Tsokos GC. Methylation status of CpG islands flanking a cAMP response element motif on the protein phosphatase 2Ac alpha promoter determines CREB binding and activity. *Journal of immunology*. 2009;182:1500–8.
- [9]. Wang T, Li J, Ding K, Zhang L, Che Q, Sun X, et al. The CpG Dinucleotide Adjacent to a kappaB Site Affects NF-kappaB Function through Its Methylation. *International journal of molecular sciences*. 2017;18.
- [10]. Murayama A, Sakura K, Nakama M, Yasuzawa-Tanaka K, Fujita E, Tateishi Y, et al. A specific CpG site demethylation in the human interleukin 2 gene promoter is an epigenetic memory. *The EMBO journal*. 2006;25:1081–92. [PubMed: 16498406]
- [11]. Luo C, Hajkova P, Ecker JR. Dynamic DNA methylation: In the right place at the right time. *Science*. 2018;361:1336–40. [PubMed: 30262495]
- [12]. Haney SL, Upchurch GM, Opavska J, Klinkebiel D, Hlady RA, Roy S, et al. Dnmt3a Is a Haploinsufficient Tumor Suppressor in CD8+ Peripheral T Cell Lymphoma. *PLoS genetics*. 2016;12:e1006334. [PubMed: 27690235]
- [13]. Kala R, Tollefsbol TO. A Novel Combinatorial Epigenetic Therapy Using Resveratrol and Pterostilbene for Restoring Estrogen Receptor-alpha (ERalpha) Expression in ERalpha-Negative Breast Cancer Cells. *PLoS one*. 2016;11:e0155057. [PubMed: 27159275]
- [14]. Papoutsis AJ, Borg JL, Selmin OI, Romagnolo DF. BRCA-1 promoter hypermethylation and silencing induced by the aromatic hydrocarbon receptor-ligand TCDD are prevented by resveratrol in MCF-7 cells. *The Journal of nutritional biochemistry*. 2012;23:1324–32. [PubMed: 22197621]
- [15]. Zhu W, Qin W, Zhang K, Rottinghaus GE, Chen YC, Kliethermes B, et al. Trans-resveratrol alters mammary promoter hypermethylation in women at increased risk for breast cancer. *Nutrition and cancer*. 2012;64:393–400. [PubMed: 22332908]
- [16]. Stefanska B, Salame P, Bednarek A, Fabianowska-Majewska K. Comparative effects of retinoic acid, vitamin D and resveratrol alone and in combination with adenosine analogues on methylation and expression of phosphatase and tensin homologue tumour suppressor gene in breast cancer cells. *The British journal of nutrition*. 2012;107:781–90. [PubMed: 21801466]
- [17]. Gracia A, Elcoroaristizabal X, Fernandez-Quintela A, Miranda J, Bediaga NG, MdP M, et al. Fatty acid synthase methylation levels in adipose tissue: effects of an obesogenic diet and phenol compounds. *Genes & nutrition*. 2014;9:411. [PubMed: 24903834]
- [18]. Zhao FQ. Octamer-binding transcription factors: genomics and functions. *Frontiers in bioscience*. 2013;18:1051–71.
- [19]. Vazquez-Arreguin K, Tantin D. The Oct1 transcription factor and epithelial malignancies: Old protein learns new tricks. *Biochimica et biophysica acta*. 2016;1859:792–804. [PubMed: 26877236]
- [20]. Hwang-Verslues WW, Chang PH, Jeng YM, Kuo WH, Chiang PH, Chang YC, et al. Loss of corepressor PER2 under hypoxia up-regulates OCT1-mediated EMT gene expression and enhances tumor malignancy. *Proceedings of the National Academy of Sciences of the United States of America*. 2013;110:12331–6. [PubMed: 23836662]
- [21]. Kalamohan K, Periasamy J, Bhaskar Rao D, Barnabas GD, Ponnaiyan S, Ganesan K. Transcriptional coexpression network reveals the involvement of varying stem cell features with different dysregulations in different gastric cancer subtypes. *Molecular oncology*. 2014;8:1306–25. [PubMed: 24917244]
- [22]. Han W, Shi M, Spivack SD. Site-specific methylated reporter constructs for functional analysis of DNA methylation. *Epigenetics : official journal of the DNA Methylation Society*. 2013;8:1176–87.

- [23]. Kislouk T, Cramer T, Meiri N. Methyl CpG level at distal part of heat-shock protein promoter HSP70 exhibits epigenetic memory for heat stress by modulating recruitment of POU2F1-associated nucleosome-remodeling deacetylase (NuRD) complex. *Journal of neurochemistry*. 2017;141:358–72. [PubMed: 28278364]
- [24]. Jafek JL, Shakya A, Tai PY, Ibarra A, Kim H, Maddox J, et al. Transcription factor Oct1 protects against hematopoietic stress and promotes acute myeloid leukemia. *Experimental hematology*. 2019;76:38–48 e2. [PubMed: 31295506]
- [25]. Wang P, Sang S. Metabolism and pharmacokinetics of resveratrol and pterostilbene. *BioFactors*. 2018;44:16–25. [PubMed: 29315886]
- [26]. Brown SE, Suderman MJ, Hallett M, Szyf M. DNA demethylation induced by the methyl-CpG-binding domain protein MBD3. *Gene*. 2008;420:99–106. [PubMed: 18602768]
- [27]. Vogel Ciernia A, Laufer BI, Hwang H, Dunaway KW, Mordaunt CE, Coulson RL, et al. Epigenomic Convergence of Neural-Immune Risk Factors in Neurodevelopmental Disorder Cortex. *Cerebral cortex*. 2020;30:640–55. [PubMed: 31240313]
- [28]. Laufer BI, Hwang H, Vogel Ciernia A, Mordaunt CE, LaSalle JM. Whole genome bisulfite sequencing of Down syndrome brain reveals regional DNA hypermethylation and novel disorder insights. *Epigenetics : official journal of the DNA Methylation Society*. 2019;14:672–84.
- [29]. MARTIN M Cutadapt removes adapter sequences from high-throughput sequencing reads. . *EMBnetjournal*, [SI] 2011;v. 17:p. pp. 10–2.
- [30]. Li H, Durbin R. Fast and accurate short read alignment with Burrows-Wheeler transform. *Bioinformatics*. 2009;25:1754–60. [PubMed: 19451168]
- [31]. Zhang Y, Liu T, Meyer CA, Eeckhoutte J, Johnson DS, Bernstein BE, et al. Model-based analysis of ChIP-Seq (MACS). *Genome biology*. 2008;9:R137. [PubMed: 18798982]
- [32]. Thomas R, Thomas S, Holloway AK, Pollard KS. Features that define the best ChIP-seq peak calling algorithms. *Briefings in bioinformatics*. 2017;18:441–50. [PubMed: 27169896]
- [33]. Ernst J, Kheradpour P, Mikkelsen TS, Shores N, Ward LD, Epstein CB, et al. Mapping and analysis of chromatin state dynamics in nine human cell types. *Nature*. 2011;473:43–9. [PubMed: 21441907]
- [34]. Perez-Pinera P, Kocak DD, Vockley CM, Adler AF, Kabadi AM, Polstein LR, et al. RNA-guided gene activation by CRISPR-Cas9-based transcription factors. *Nature methods*. 2013;10:973–6. [PubMed: 23892895]
- [35]. Schmid-Burgk JL, Honing K, Ebert TS, Hornung V. CRISPaint allows modular base-specific gene tagging using a ligase-4-dependent mechanism. *Nature communications*. 2016;7:12338.
- [36]. Rivero-Gutiérrez B, Anzola A, Martínez-Augustín O, de Medina FS. Stain-free detection as loading control alternative to Ponceau and housekeeping protein immunodetection in Western blotting. *Analytical biochemistry*. 2014;467:1–3. [PubMed: 25193447]
- [37]. Figueroa DM, Darrow EM, Chadwick BP. Two novel DXZ4-associated long noncoding RNAs show developmental changes in expression coincident with heterochromatin formation at the human (*Homo sapiens*) macrosatellite repeat. *Chromosome research : an international journal on the molecular, supramolecular and evolutionary aspects of chromosome biology*. 2015;23:733–52.
- [38]. Chadwick BP. DXZ4 chromatin adopts an opposing conformation to that of the surrounding chromosome and acquires a novel inactive X-specific role involving CTCF and antisense transcripts. *Genome research*. 2008;18:1259–69. [PubMed: 18456864]
- [39]. Johnston JR, Chase PB, Pinto JR. Troponin through the looking-glass: emerging roles beyond regulation of striated muscle contraction. *Oncotarget*. 2018;9:1461–82. [PubMed: 29416706]
- [40]. Suzuki IK, Gacquer D, Van Heurck R, Kumar D, Wojno M, Bilheu A, et al. Human-Specific NOTCH2NL Genes Expand Cortical Neurogenesis through Delta/Notch Regulation. *Cell*. 2018;173:1370–84 e16. [PubMed: 29856955]
- [41]. Wang Y, Zhou J, Wang Z, Wang P, Li S. Upregulation of SOX2 activated LncRNA PVT1 expression promotes breast cancer cell growth and invasion. *Biochemical and biophysical research communications*. 2017;493:429–36. [PubMed: 28882595]

- [42]. Tang T, Guo C, Xia T, Zhang R, Zen K, Pan Y, et al. LncCCAT1 Promotes Breast Cancer Stem Cell Function through Activating WNT/beta-catenin Signaling. *Theranostics*. 2019;9:7384–402. [PubMed: 31695775]
- [43]. Soll JM, Brickner JR, Mudge MC, Mosammaparast N. RNA ligase-like domain in activating signal cointegrator 1 complex subunit 1 (ASCC1) regulates ASCC complex function during alkylation damage. *The Journal of biological chemistry*. 2018;293:13524–33. [PubMed: 29997253]
- [44]. Gabay M, Li Y, Felsher DW. MYC activation is a hallmark of cancer initiation and maintenance. *Cold Spring Harbor perspectives in medicine*. 2014;4.
- [45]. Cooke M, Magimaidas A, Casado-Medrano V, Kazanietz MG. Protein kinase C in cancer: The top five unanswered questions. *Molecular carcinogenesis*. 2017;56:1531–42. [PubMed: 28112438]
- [46]. Makuuchi R, Terashima M, Kusuhara M, Nakajima T, Serizawa M, Hatakeyama K, et al. Comprehensive analysis of gene mutation and expression profiles in neuroendocrine carcinomas of the stomach. *Biomedical research*. 2017;38:19–27. [PubMed: 28239029]
- [47]. You Z, Li B, Xu J, Chen L, Ye H. Curcumin suppress the growth of hepatocellular carcinoma via down-regulating SREBF1. *Oncology research*. 2018.
- [48]. Syafruddin SE, Rodrigues P, Vojtasova E, Patel SA, Zaini MN, Burge J, et al. A KLF6-driven transcriptional network links lipid homeostasis and tumour growth in renal carcinoma. *Nature communications*. 2019;10:1152.
- [49]. Nath A, Chan C. Genetic alterations in fatty acid transport and metabolism genes are associated with metastatic progression and poor prognosis of human cancers. *Scientific reports*. 2016;6:18669. [PubMed: 26725848]
- [50]. Pham TND, Perez White BE, Zhao H, Mortazavi F, Tonetti DA. Protein kinase C alpha enhances migration of breast cancer cells through FOXC2-mediated repression of p120-catenin. *BMC cancer*. 2017;17:832. [PubMed: 29216867]
- [51]. Lonne GK, Cornmark L, Zahirovic IO, Landberg G, Jirstrom K, Larsson C. PKCalpha expression is a marker for breast cancer aggressiveness. *Molecular cancer*. 2010;9:76. [PubMed: 20398285]
- [52]. Tam WL, Lu H, Buikhuisen J, Soh BS, Lim E, Reinhardt F, et al. Protein kinase C alpha is a central signaling node and therapeutic target for breast cancer stem cells. *Cancer cell*. 2013;24:347–64. [PubMed: 24029232]
- [53]. Chik F, Szyf M. Effects of specific DNMT gene depletion on cancer cell transformation and breast cancer cell invasion; toward selective DNMT inhibitors. *Carcinogenesis*. 2011;32:224–32. [PubMed: 20980350]
- [54]. Rhee I, Bachman KE, Park BH, Jair KW, Yen RW, Schuebel KE, et al. DNMT1 and DNMT3b cooperate to silence genes in human cancer cells. *Nature*. 2002;416:552–6. [PubMed: 11932749]
- [55]. Hlady RA, Novakova S, Opavska J, Klinkebiel D, Peters SL, Bies J, et al. Loss of Dnmt3b function upregulates the tumor modifier Ment and accelerates mouse lymphomagenesis. *The Journal of clinical investigation*. 2012;122:163–77. [PubMed: 22133874]
- [56]. Zheng Y, Zhang H, Wang Y, Li X, Lu P, Dong F, et al. Loss of Dnmt3b accelerates MLL-AF9 leukemia progression. *Leukemia*. 2016;30:2373–84. [PubMed: 27133822]
- [57]. Peralta-Arrieta I, Hernandez-Sotelo D, Castro-Coronel Y, Leyva-Vazquez MA, Illades-Aguir B. DNMT3B modulates the expression of cancer-related genes and downregulates the expression of the gene VAV3 via methylation. *American journal of cancer research*. 2017;7:77–87. [PubMed: 28123849]
- [58]. Tseng LL, Cheng HH, Yeh TS, Huang SC, Syu YY, Chuu CP, et al. Targeting the histone demethylase PHF8-mediated PKCalpha-Src-PTEN axis in HER2-negative gastric cancer. *Proceedings of the National Academy of Sciences of the United States of America*. 2020;117:24859–66. [PubMed: 32958674]
- [59]. Schlesinger Y, Straussman R, Keshet I, Farkash S, Hecht M, Zimmerman J, et al. Polycomb-mediated methylation on Lys27 of histone H3 pre-marks genes for de novo methylation in cancer. *Nature genetics*. 2007;39:232–6. [PubMed: 17200670]

- [60]. Hagemann S, Kuck D, Stresemann C, Prinz F, Brueckner B, Mund C, et al. Antiproliferative effects of DNA methyltransferase 3B depletion are not associated with DNA demethylation. *PLoS one*. 2012;7:e36125. [PubMed: 22563479]
- [61]. Micevic G, Muthusamy V, Damsky W, Theodosakis N, Liu X, Meeth K, et al. DNMT3b Modulates Melanoma Growth by Controlling Levels of mTORC2 Component RICTOR. *Cell reports*. 2016;14:2180–92. [PubMed: 26923591]
- [62]. Tavakolian S, Goudarzi H, Faghiloo E. E-cadherin, Snail, ZEB-1, DNMT1, DNMT3A and DNMT3B expression in normal and breast cancer tissues. *Acta biochimica Polonica*. 2019;66:409–14. [PubMed: 31880901]
- [63]. Jahangiri R, Jamialahmadi K, Gharib M, Emami Razavi A, Mosaffa F. Expression and clinicopathological significance of DNA methyltransferase 1, 3A and 3B in tamoxifen-treated breast cancer patients. *Gene*. 2019;685:24–31. [PubMed: 30359738]
- [64]. Gagliardi M, Strazzullo M, Matarazzo MR. DNMT3B Functions: Novel Insights From Human Disease. *Frontiers in cell and developmental biology*. 2018;6:140. [PubMed: 30406101]
- [65]. Li W, Yi J, Zheng X, Liu S, Fu W, Ren L, et al. miR-29c plays a suppressive role in breast cancer by targeting the TIMP3/STAT1/FOXO1 pathway. *Clinical epigenetics*. 2018;10:64. [PubMed: 29796115]
- [66]. Erasalo H, Hamalainen M, Leppanen T, Maki-Opas I, Laavola M, Haavikko R, et al. Natural Stilbenoids Have Anti-Inflammatory Properties in Vivo and Down-Regulate the Production of Inflammatory Mediators NO, IL6, and MCP1 Possibly in a PI3K/Akt-Dependent Manner. *Journal of natural products*. 2018;81:1131–42. [PubMed: 29726680]
- [67]. O'Hagan HM, Wang W, Sen S, Destefano Shields C, Lee SS, Zhang YW, et al. Oxidative damage targets complexes containing DNA methyltransferases, SIRT1, and polycomb members to promoter CpG Islands. *Cancer cell*. 2011;20:606–19. [PubMed: 22094255]
- [68]. Maiuri AR, Peng M, Podicheti R, Sriramkumar S, Kamplain CM, Rusch DB, et al. Mismatch Repair Proteins Initiate Epigenetic Alterations during Inflammation-Driven Tumorigenesis. *Cancer research*. 2017;77:3467–78. [PubMed: 28522752]
- [69]. Beetch M, Harandi-Zadeh S, Shen K, Lubecka K, Kitts DD, O'Hagan HM, et al. Dietary antioxidants remodel DNA methylation patterns in chronic disease. *British journal of pharmacology*. 2020;177:1382–408. [PubMed: 31626338]
- [70]. Lehnertz B, Ueda Y, Derijck AA, Braunschweig U, Perez-Burgos L, Kubicek S, et al. Suv39h-mediated histone H3 lysine 9 methylation directs DNA methylation to major satellite repeats at pericentric heterochromatin. *Current biology : CB*. 2003;13:1192–200. [PubMed: 12867029]
- [71]. Maddox J, Shakya A, South S, Shelton D, Andersen JN, Chidester S, et al. Transcription factor Oct1 is a somatic and cancer stem cell determinant. *PLoS genetics*. 2012;8:e1003048. [PubMed: 23144633]
- [72]. Shin HJ, Park HY, Jeong SJ, Park HW, Kim YK, Cho SH, et al. STAT4 expression in human T cells is regulated by DNA methylation but not by promoter polymorphism. *Journal of immunology*. 2005;175:7143–50.

**Highlights:**

- Pterostilbene leads to DNA methylation and silencing of oncogenes
- Pterostilbene leads the recruitment of DNMT3B to oncogenes
- Pterostilbene-mediated DNA methylation and silencing of oncogenes is DNMT3B-dependent
- DNA hypermethylation observed upon PTS treatment is not signalled by OCT1-reduced binding

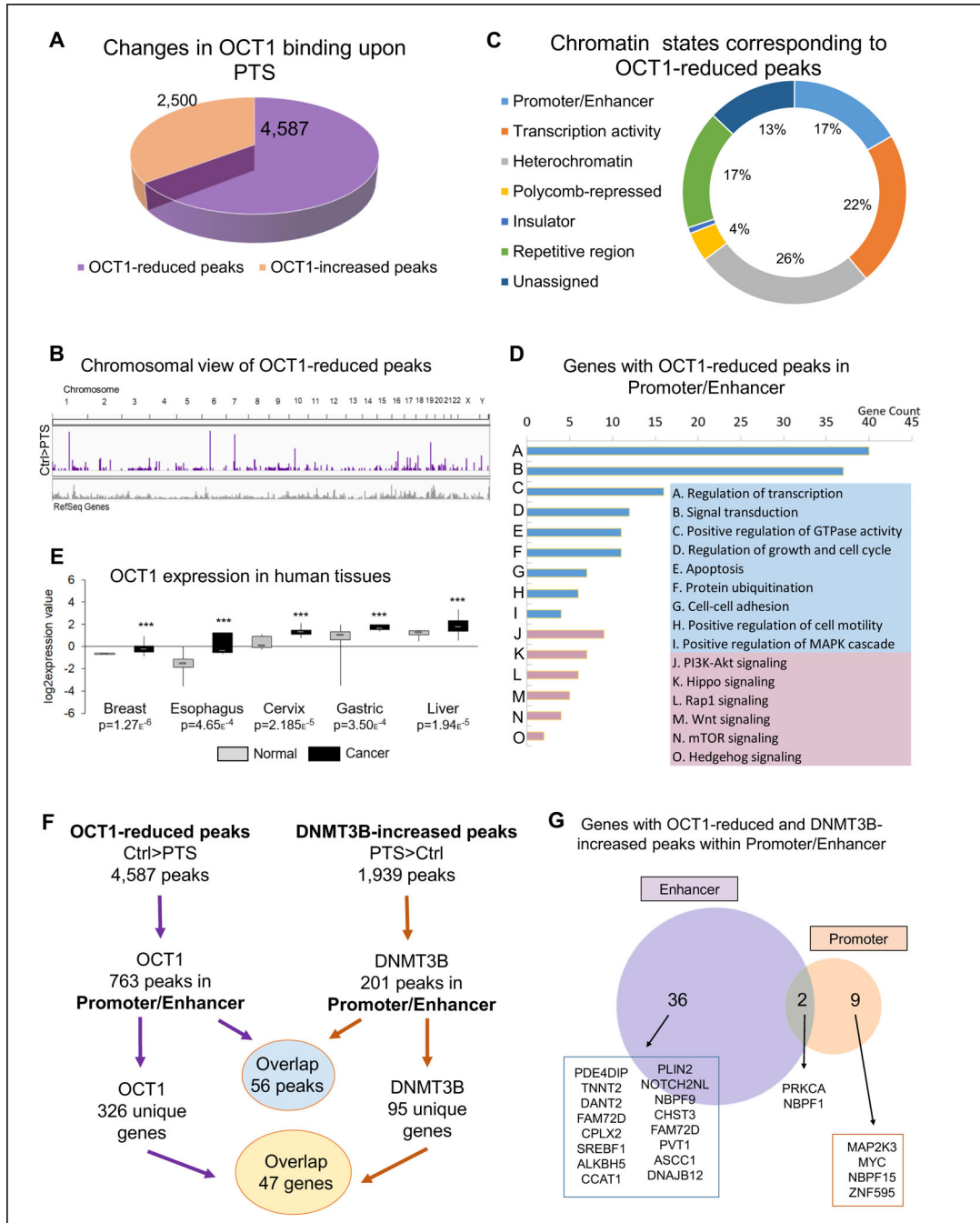


**Figure 1. Overview of genome-wide changes of OCT1 binding in response to PTS.** (A) A pie chart depicting the number of changes in OCT1 binding in MCF10CA1a breast cancer cells treated with 7µM PTS for 9 days. OCT1 binding was assessed by ChIP sequencing. (B) Chromosomal view of OCT1-reduced peaks in response to PTS treatment. Each bar represents a single peak that was called using MACS2 peak calling software. (C) Chromatin states associated with OCT1-reduced peaks were determined using Broad ChromHMM data from human mammary epithelial cells (HMEC) available on USCS Genome Browser (hg19). Peaks could correspond to active, weak or poised

promoters, strong or weak enhancers, putative insulators, active or weak transcription, Polycomb-repressed regions, heterochromatin or repetitive regions. (D) The 326 genes with OCT1-reduced peaks in promoter/enhancer regions upon PTS were subjected to Gene Ontology (GO) function (blue color) and Kyoto Encyclopedia of Genes and Genomes (KEGG) pathway analysis (pink color) using DAVID Knowledgebase. The number of genes in different categories is depicted in a chart. (E) OCT1 expression in normal and cancer tissues based on microarray data from Oncomine database. Expression is presented as log<sub>2</sub>-transformed median centered per array, and SD-normalized to 1 per array. (F) Schematic of analysis of peaks and genes associated with OCT1-reduced and DNMT3B-enriched peaks within promoter/enhancer in MCF10CA1a breast cancer cells treated with 7 $\mu$ M PTS for 9 days. (G) The 47 genes with DNMT3B enrichment in OCT1-reduced peaks in promoter/enhancer in response to PTS were categorized into genes containing promoter peaks only, promoter and enhancer peaks, or enhancer peaks only as depicted by the Venn diagram. Selected genes with known or potential oncogenic role that are associated with those peaks are listed.

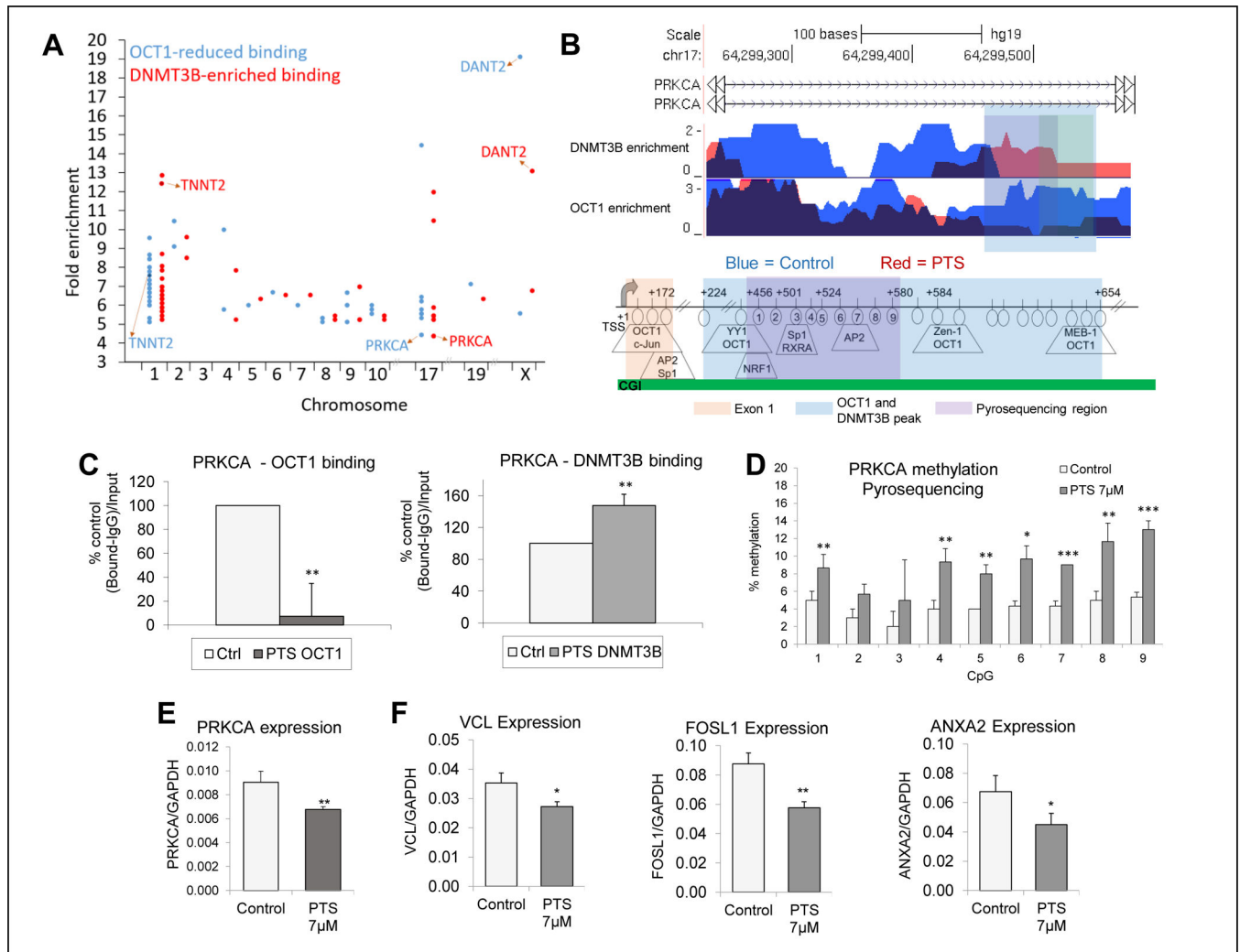


**Figure 2. Hypermethylation of *PRKCA* in OCT1-reduced and DNMT3B-enriched region is linked to *PRKCA* transcriptional silencing in response to PTS in breast cancer cells.**

(A) A chart depicting 56 peaks that overlap between OCT1-reduced and DNMT3B-enriched binding with their chromosomal location and ChIP-seq fold change in MCF10CA1a breast cancer cells treated with 7  $\mu$ M PTS for 9 days as compared with vehicle-treated cells. (B) Genome browser tracks depicting DNMT3B and OCT1 enrichment in binding within *PRKCA* promoter region in vehicle-treated (blue, control) and PTS-treated (red) MCF10CA1a breast cancer cells. The blue-shaded track region represents the OCT1-reduced and DNMT3B-increased overlapping peaks. Below the tracks, gene maps are depicted with transcription start site (TSS) indicated by +1, transcription factors predicted using Transfac, and pyrosequenced CpG sites circled and numbered. (C) Binding of OCT1 and DNMT3B at *PRKCA* promoter region, as determined by quantitative ChIP, in MCF10CA1a breast cancer cells treated with 7 $\mu$ M PTS. (D) Average methylation status of CpG sites within *PRKCA* promoter as determined by pyrosequencing in MCF10CA1a breast cancer cells treated for 9 days with 7 $\mu$ M PTS. (E) *PRKCA* gene expression upon 9-day treatment of MCF10CA1a breast cancer cells with 7 $\mu$ M PTS as determined by qPCR. (F) Expression of PKC- $\alpha$ -target genes, *VCL*, *FOSL1* and *ANXA2*, upon 9-day treatment

of MCF10CA1a breast cancer cells with 7 $\mu$ M PTS as determined by qPCR. All results represent mean  $\pm$  SD of three independent experiments; \*\*\*P<0.001, \*\*P<0.01, \*P<0.05.

Author Manuscript

Author Manuscript

Author Manuscript

Author Manuscript

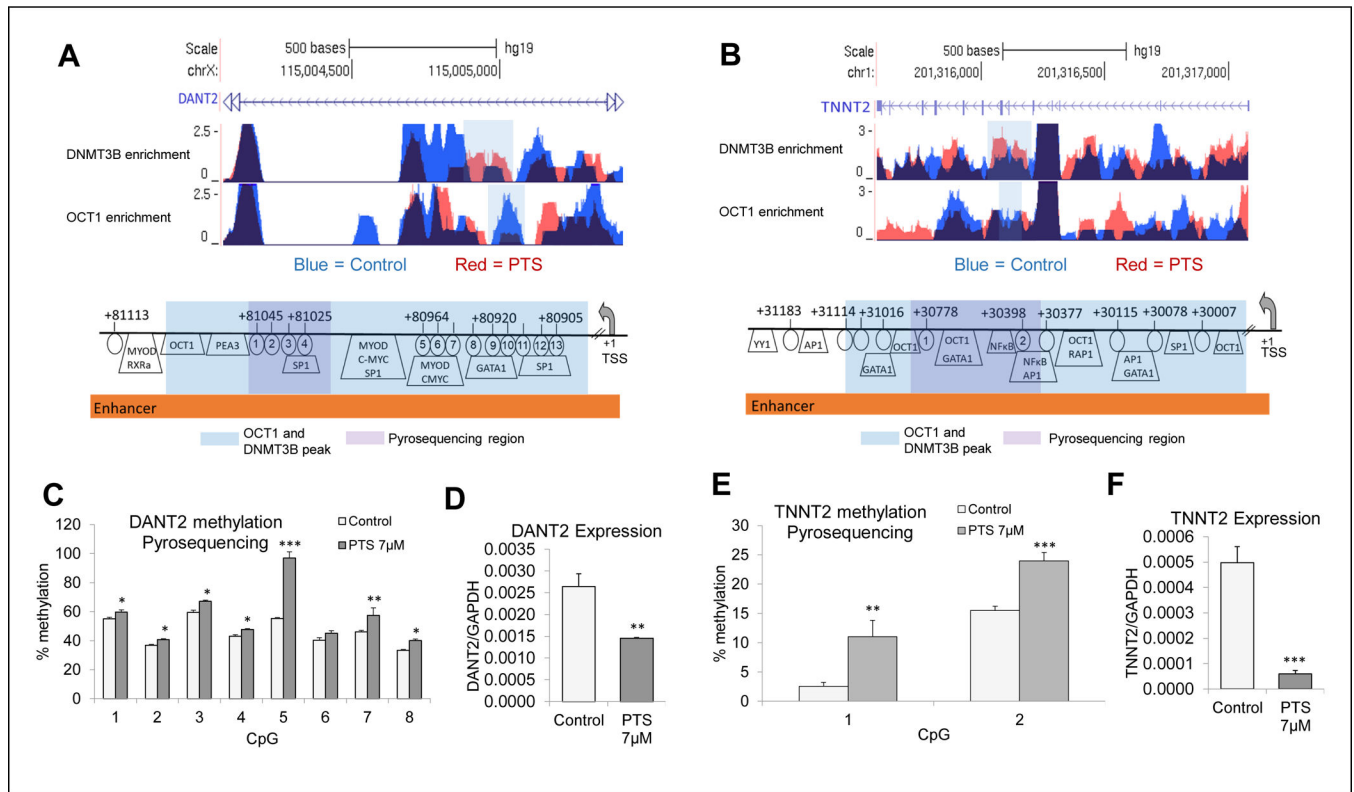


**Figure 3. Hypermethylation of *DANT2* and *TNNT2* in *OCT1*-reduced and *DNMT3B*-enriched region is linked to their transcriptional silencing in response to PTS in breast cancer cells.** (A, B) Genome browser tracks depicting *DNMT3B* and *OCT1* enrichment in binding within *DANT2* and *TNNT2* enhancer regions in vehicle-treated (blue, control) and PTS-treated (red) MCF10CA1a breast cancer cells. The blue-shaded track region represents the *OCT1*-reduced and *DNMT3B*-increased overlapping peaks. Below the tracks, gene maps are depicted with transcription start site (TSS) indicated by +1, transcription factors predicted using Transfac, and pyrosequenced CpG sites circled and numbered. (C, E) Average methylation status of CpG sites within *DANT2* and *TNNT2* enhancer regions as determined by pyrosequencing in MCF10CA1a breast cancer cells treated for 9 days with 7 $\mu$ M PTS. (D, F) *DANT2* and *TNNT2* gene expression upon 9-day treatment of MCF10CA1a breast cancer cells with 7 $\mu$ M PTS as determined by qPCR. All results represent mean  $\pm$  SD of three independent experiments; \*\*\*P<0.001, \*\*P<0.01, \*P<0.05.

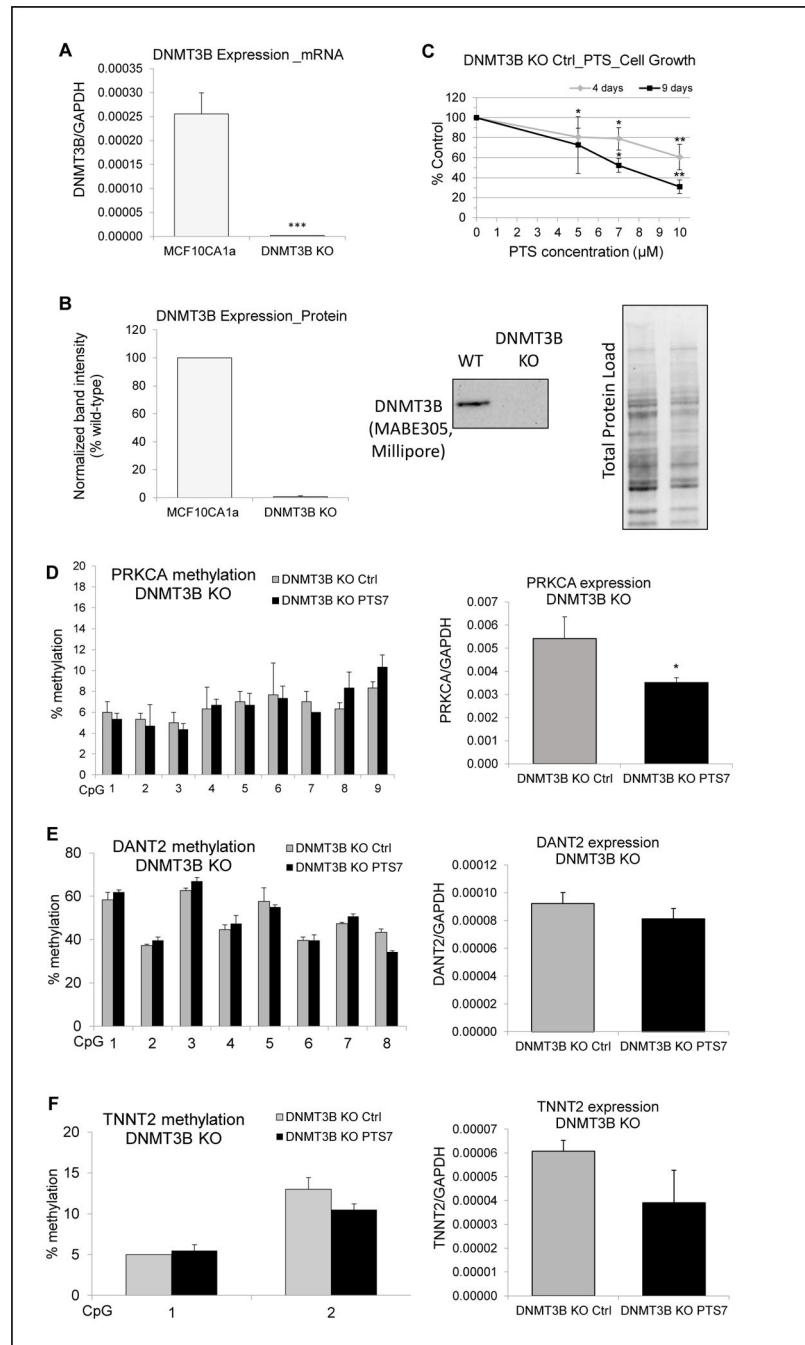


**Figure 4. DNMT3B-dependent hypermethylation of *PRKCA*, *DANT2*, and *TNNT2* in response to PTS.**

(A, B) *DNMT3B* gene expression at mRNA (A) and protein levels (B) in *DNMT3B* knockout cells (DNMT3B KO), as determined by qPCR and western blot, respectively. In western blot analyses, reactive bands were visualized using the chemiluminescent protocol in the ChemiDoc MP Imaging System (Bio-Rad) and analyzed using the Image Lab software. Protein loading was normalized with respect to total sample protein loaded using free stain gels. (C) Cell growth of DNMT3B KO cells in response to 4- and 9-day treatment with 5 $\mu$ M, 7 $\mu$ M, and 10 $\mu$ M PTS, as determined by trypan blue exclusion test. (D, E, F)

Average methylation status of CpG sites within *PRKCA* promoter, and *DANT2* and *TNNT2* enhancers, as determined by pyrosequencing, in DNMT3B KO cells treated with vehicle (ethanol, DNMT3B KO Ctrl) or with 7 $\mu$ M PTS for 9 days (DNMT3B KO PTS7). Right panel depicts expression of *PRKCA* (D), *DANT2* (E), and *TNNT2* (F) in DNMT3B KO Ctrl cells and DNMT3B KO PTS7 cells, as determined by qPCR. All results represent mean  $\pm$  SD of three independent experiments; \*\*\*P<0.001, \*\*P<0.01, \*P<0.05.

Author Manuscript

Author Manuscript

Author Manuscript

Author Manuscript